Coulomb effects on the quantum cyclotron resonance from a two-dimensional electron liquid with extremely narrow Landau levels

Yu. P. Monarkha
Grenoble High Magnetic Field Laboratory, MPI - FKF and CNRS, Boîte Postale 166, F-38042 Grenoble Cedex 9, France
and Institute for Low Temperature Physics and Engineering, 47 Lenin avenue, 310164 Kharkov, Ukraine

E. Teske and P. Wyder
Grenoble High Magnetic Field Laboratory, MPI - FKF and CNRS, Boîte Postale 166, F-38042 Grenoble Cedex 9, France
(Received 18 February 2000)

We report results of experimental and theoretical studies of cyclotron resonance (CR) absorption from a strongly interacting nondegenerate two-dimensional electron liquid with extremely narrow Landau levels realized on the free surface of liquid helium. We found that the main many-electron effect on the quantum CR originates from the ultrafast fluctuational motion of electron orbit centers, causing inelastic scattering in the moving frames. This effect is described by means of the memory function formalism, employing a many-electron approximation for the electron dynamic structure factor (DSF). Remarkably, the Coulombic effect leads to a narrowing of Landau levels and at the same time produces a strong broadening of the electron DSF and the relaxation kernel of the dynamic conductivity. This explains the observed transformation of the CR line shape and the successive narrowing and broadening of the CR linewidth with the increase of the electron density. It is shown that the Coulomb narrowing and broadening of the CR data respond differently to a change of the resonant frequency in accordance with the concept proposed.

I. INTRODUCTION

Considerable research has been performed on cyclotron resonance (CR) in two-dimensional (2D) electron systems created in semiconductor structures, and on the free surface of superfluid helium. The fundamental interest of CR studies in such systems is based on the singular nature of a 2D electron gas in the presence of a strong normal magnetic field.[1,2] For an ideal 2D electron gas the electron energy spectrum is discrete, $\varepsilon_N=\hbar\omega_c(N+1/2)$, and the effect of collision broadening of Landau levels must be treated self-consistently.[3] The finite CR linewidth γ as well as the finite dc magnetoconductivity $\sigma_{xx}(0)$ result from electron scattering within the Landau levels broadened due to interaction with scatterers.[4] Additionally, the effects of electron-electron interaction are usually stronger for 2D electrons with narrow Landau levels.

In semiconductor 2D electron systems at low temperatures, electrons form a degenerate electron gas. Interesting many-electron effects on the CR from Si inversion layers were observed in Refs. 5–7, when the lowest Landau level is partially occupied. At the smallest electron densities achieved in these studies, $n_s\sim 5\times 10^9$ cm^{-2}, the CR linewidth is much narrower than it could be, according to any single-electron theory or the semiclassical Drude formula. The linewidth broadens with the increase of electron density n_s, and attains a maximum when the ground Landau level is completely filled.[6,7] A further narrowing of the CR absorption with the increase of n_s, observed for filling factors $\nu_{\rm fill}>1$, was explained in Ref. 8 by means of a self-consistent improvement of the random-phase approximation (RPA). The origin of the strong narrowing of the CR linewidth observed at $\nu_{\rm fill}<1$ was attributed first to charge-density-wave pinning,[6] then to a magnetic field-induced Wigner glass.[7] The same effect of CR narrowing with the decrease of n_s observed for the GaAs 2D electron gas had been presented in Ref. 9 as a manifestation of the strong influence of electron-electron interactions on the CR line. Qualitative explanations of the unusually narrow CR were based on the magnetoplasmon interaction model of Kallin and Halperin,[10] though it was established for integral values of $\nu_{\rm fill}$.

A remarkable 2D electron system is formed on the free surface of liquid helium.[11] This model system is characterized by the uniquely strong Coulomb interaction between electrons: the mean Coulomb potential energy U_C can be 100 times larger than the mean kinetic energy k_BT (here the Fermi energy is much smaller than the thermal energy). Though the filling factor is usually very small in strong magnetic fields ($\hbar\omega_c>k_BT$) and the electrons form a nondegenerate system, the Landau-level broadening induced by scatterers is extremely weak, $\Gamma_N\ll k_BT$. The latter means that, in spite of the considerable thermal energy, electrons are confined to a very narrow energy range near the positions of the unperturbed Landau levels. Extremely narrow Landau levels cause an interesting inelastic effect on the dc magnetotransport of surface electrons (SE's), when the energy exchange at a collision exceeds the level broadening Γ_N.[12] Under the conditions $\Gamma_N\ll k_BT\ll U_C$, a strong influence of electron-electron interactions on the CR is also expected. Therefore, this model system can be used for testing different theoretical approaches to the quantum CR of highly correlated 2D electrons.

In degenerate 2D electron systems of semiconductors, the single-electron approach is applicable in the high-electron-density regime, and lowering n_s introduces Coulomb corre-

lations. As for SE's on helium, this nondegenerate electron system is on the other side of the phase diagram, and lowering n_s makes the single-electron approximation more applicable, while an increase of electron density enhances many-electron effects. Thus, contrary to the semiconductor systems, SE's on liquid helium allow one to study the appearance of Coulomb effects on the CR absorption with the increase of n_s, starting from the smallest densities $n_s \sim 10^7$ cm^{-2} ($\nu_{\rm fill} \ll 1$), where the single-electron approximation does not interfere with the effect of completion of the ground Landau level. Comparing experimental data obtained from such a pure system with different theoretical models can reveal the origin of a strong CR narrowing induced by electron-electron interactions.

For SE's on liquid helium there are two kinds of scatterers: vapor atoms of ^{4}He above the liquid surface, and capillary wave quanta (ripplons). We confine ourselves to the electron-vapor atom scattering which dominates at $T > 1$ K. Vapor atoms are relatively slow, and their interaction with electrons can be considered like a short-range impurity interaction in solids. In the laboratory frame, the electron-vapor atom scattering can be described as an elastic one, since the energy exchange $\hbar \Delta\omega$ is much smaller than Γ_N. The density of these ''impurities'' $n^{(a)}$ decreases exponentially with cooling which is the cause of extremely narrow Landau levels. The interaction potential has the most simple form $V_{\rm int} = U_a \delta(\mathbf{R}_e - \mathbf{R}_a)$, which has been frequently employed in different theoretical models of many-body physics.

CR experiments with SE's on helium, performed long ago,[13,14] showed the effect of quantization of both out-of-plane and in-plane motions on electron transport phenomena. Regarding many-electron effects on the CR, until recently, the experimental situation (reviewed in Ref. 15) is very complicated, unclear, and challenging.

Recently,[15] we briefly reported the observation of Coulomb narrowing of the CR linewidth for the electron-vapor atom scattering regime for low enough electron densities. This behavior was in qualitative agreement with the main result of the many-electron theory of Dykman and Khazan (DK).[16] According to this theory, the fluctuational many-electron electric field $\mathbf{E}_f$ acting on each electron can be approximately considered as a quasiuniform field causing a continuous correction to the Landau spectrum eE_fX (here X is the electron orbit center coordinate along the field). The narrowing of the CR linewidth $\gamma \propto 1/n_s^{3/4}$ (Refs. 16 and 17) is the result of the kinetics of 2D electrons with the continuous spectrum correction. However, the experimental density dependence of the CR linewidth appeared to be more complicated than this straight decrease.[15] First, in the low-electron-density range ($n_s \sim 0.1 \times 10^8$ cm^{-2}), the Coulomb narrowing is substantially weaker than the prediction of the DK theory. It achieves the predicted rate only at medium densities $n_s \sim 0.8 \times 10^8$ cm^{-2}. Then, at $n_s > 2 \times 10^8$ cm^{-2}, the Coulomb effect changes sign, and a strong increase of the CR linewidth with electron density was observed in accordance with previous measurements.[14,18]

The presence of the strong many-electron fluctuational field $\mathbf{E}_f$ results in ultrafast drift velocities of the electron orbit centers $u_f = cE_f/B$. According to the analysis presented in Refs. 15, it is the fast drift velocities of the electron orbit centers that strongly affect the quantum magnetotransport of SE's. For each electron, there is only one reference frame, where it has the discrete Landau spectrum: the frame that moves along with the electron orbit center. In this frame, the energy exchange at a collision between an electron and an impurity is no longer zero, since the impurity hits the electron orbit with the velocity $-\mathbf{u}_f$ and the energy exchange attains the well known Doppler shift correction $\hbar \mathbf{q} \cdot \mathbf{u}_f$. The appearance of the energy exchange $\hbar \mathbf{q} \cdot \mathbf{u}_f$ produces two effects:[15] (1) the suppression of electron scattering within the Landau levels, if $\hbar \mathbf{q} \cdot \mathbf{u}_f > \Gamma_N$; and (2) the stimulation of electron scattering between different Landau levels, if $\hbar \mathbf{q} \cdot \mathbf{u}_f \gtrsim \hbar \omega_c$. Since $\hbar \omega_c \gg \Gamma_N$, these two effects are quite separated on the n_s axis. In the single-electron approach, for electron scattering within the Landau levels, the CR linewidth is determined by the Landau-level broadening itself.[4] Therefore, the suppression of electron scattering under CR conditions can be also described as a Coulomb narrowing of Landau levels.[15] This allows one to explain the narrowing of the CR linewidth with the increase of electron density observed. The stimulation of electron scattering between different Landau levels increases the collision broadening of the Landau levels due to the mixing of levels, though this increase cannot describe the experimentally observed increase of the CR linewidth.

In this paper, we present a many-electron theory of quantum CR from a nondegenerate 2D electron liquid with extremely narrow Landau levels, and the results of a detailed experimental study of the many-electron effects on the CR absorption from SE's on superfluid helium. The CR data, measured for different resonant frequencies, show the successive strong narrowing and broadening of the CR linewidth with the increase of electron density. We found that the Coulomb narrowing and broadening of the CR linewidth respond differently to an increase of the resonant frequency, which allows one to check the theoretical concept of the many-electron effect.

Contrary to the semiconductor systems, our studies correspond to the density range where the theoretical results of Ref. 8 are not applicable. Our theory is based on the general result of the memory function formalism,[2,19,20] which establishes the relation between the relaxation kernel $M(\omega)$ [or the frequency-dependent width $\gamma_L(\omega) = 2{\rm Im}M(\omega)$ of a Lorentzian absorption function] and the equilibrium electron dynamic structure factor (DSF) $S_0(q,\omega)$. Since the RPA cannot be employed here, to incorporate the many-electron effect in the electron DSF we propose an approach which takes into account the ultrafast motion of electron orbit centers. This approximation takes into account that each electron has the free-electron Landau spectrum in its own frame, which moves ultrafast $\hbar \mathbf{q} \cdot \mathbf{u}_f > \Gamma_N$ relative to the electron liquid center-of-mass frame, due to the fluctuational field. As compared to the DK theory,[16,17] we avoid the introduction of a continuous electron spectrum correction, eliminating the fluctuational electric field by means of the transcription into the local frames, moving ultrafast along with each electron orbit center. This allows us to describe the interplay of the many-electron effect and collision broadening disregarded previously, and to extend the many-electron CR theory substantially. We found that the same many-electron effect that narrows Landau levels with the increase of electron density produces a strong broadening of the electron DSF $S_0(q,\omega)$

and frequency-dependent width parameter $\gamma_L(\omega)$ as functions of $\omega - N\omega_c$. This allows us to describe both many-electron effects (narrowing and broadening of the CR) induced by the energy exchange $\hbar\mathbf{q}\cdot\mathbf{u}_f$ in the same way, and to explain the observed line-shape transformation from the pure Gaussian of the low- n_s regime to the pure Lorentzian of the high-n_s regime. Contrary to the previously used density-dependent Landau-level width model, our theory gives a proper description of the Coulomb broadening of the CR, which even numerically agrees with the experimental data. The CR studies performed here may also explain the intriguing narrowing of the CR linewidth reported for semiconductor 2D electron systems.

II. THEORETICAL CONCEPT

The distribution of the many-electron fluctuational field $\mathbf{E}_f$, acting on an electron, was found in Ref. 17. Of course, for an isotropic liquid, the direction of $\mathbf{E}_f$ is randomly distributed within the electron layer. The distribution of absolute values E_f can be approximately described as a Gaussian function with $\sqrt{\langle E_f^2\rangle} \equiv E_f^{(0)} \simeq 0.84\sqrt{4\pi k_B T_e n_s^{3/2}}$. The fluctuational electric field can be treated as an uniform field, if $\Delta_f \equiv eE_f l < k_B T_e$ (here $l = \sqrt{\hbar c/eB}$ is the magnetic length). We assume these properties of the many-electron internal field as well established.

Thus the problem of strongly interacting electrons can be reduced to a description of noninteracting electrons exposed to the fluctuational quasiuniform electric field $\mathbf{E}_f^{(i)}$ distributed accordingly. Each electron orbit drifts in crossed magnetic and fluctuational electric fields with the velocity $\mathbf{u}_f^{(i)}$ relative to the center-of-mass frame of the whole electron liquid. It should be emphasized that the quasiuniform fluctuational field does not change the singular nature of the 2D electron system in the normal magnetic field, since this field can be eliminated by a proper choice of the reference frame $\mathbf{E}_f' = \mathbf{E}_f - \frac{1}{2}\mathbf{B}\times\mathbf{u} \to 0$. This is the frame where the center of the electron orbit is at rest and the electron spectrum coincides with the discrete Landau spectrum. If electron scattering is described in this frame, we still need to introduce the Landau-level broadening in the self-consistent way, since the strength of the many-electron effect depends strongly on the relation between Δ_f and Γ_N. For the dc magnetoconductivity,[21] this transcription allows one to incorporate naturally the many-electron effect with the self-consistent Born approximation (SCBA). As for the CR theory, there are two approaches which benefit from a transcription into the frames moving along with the electron orbit centers.

A. Density-dependent Landau-level width approach

Regarding electron scattering induced by impurities, at $\hbar\mathbf{q}\cdot\mathbf{u}_f \sim \Delta_f > \Gamma_N$, the drift velocity of an electron orbit is ultrafast, since it strongly affects the probability of scattering. As for electron transitions induced by the microwave radiation, the velocities u_f are too slow to be taken into account in a direct way. Therefore, as a first approximation we can consider the CR theory of independent electrons with the Landau-level broadening $\Gamma_N(u_f)$ affected by the drift velocity u_f.

For short-range scattering, the CR theory that disregards the Coulomb interaction between electrons gives the result[4]

$$\mathrm{Re}[\sigma_{xx}(\omega)] = \frac{e^2\omega_c}{4\pi^2}\int dE[f(E) - f(E+\hbar\omega)] \times \mathrm{Im}\, G_0(E)\,\mathrm{Im}\, G_1(E+\hbar\omega), \qquad (1)$$

where $f(E)$ is the Fermi distribution function, and $G_N(E)$ is the single-electron Green's function. $\mathrm{Im}\, G_N(E)$ represents the density of states of the Landau levels. The SCBA theory results in a semielliptic Landau-level shape,[4] while the cumulant expansion method[22] yields a Gaussian level shape with the same broadening parameter Γ_N:

$$-\mathrm{Im}\, G_N(E) = (\sqrt{2\pi}/\Gamma_N)\exp[-2(E-E_N)^2/\Gamma_N^2]. \qquad (2)$$

The analysis presented in Ref. 1 shows that the Landau-level shape is close to a Gaussian for the ground Landau level, and transforms to a semielliptic shape for $N \gg 1$. It should be noted that for nondegenerate electrons, both Landau level shapes give numerically close results. We employ the Gaussian shape, since it allows us to present most of our results in an instructive analytical form.

In the ultraquantum limit, Eq. (1) yields

$$\mathrm{Re}[\sigma_{xx}(\omega)] = \frac{\sqrt{\pi}e^2 n_s \hbar}{4m\Gamma_{0,1}}\exp\left[-\frac{\hbar^2(\omega-\omega_c)^2}{\Gamma_{0,1}^2}\right], \qquad (3)$$

where we introduced the averaged broadening $\Gamma_{N,N'} = \sqrt{(\Gamma_N^2 + \Gamma_{N'}^2)/2}$. In the original SCBA theory, for short-range interaction, the Landau-level broadening does not depend on N; still we keep the subscript N, since the many-electron reduction of Γ_N strongly depends on N. The width of the CR absorption line at half-height, that follows from Eq. (3), can be written as $\gamma_G \simeq \sqrt{2}\Gamma_{0,1}/(0.849\hbar)$.

To find the Landau-level broadening as a function of the drift velocity of the electron orbit, we use the conventional perturbation procedure which employs the Green's function of scatterers $D(q,t-t')$. In our case, the scatterers are helium vapor atoms described by the many-body operators $a_{\mathbf{K}}^\dagger$ and $a_{\mathbf{K}}$ (here $\mathbf{K}=\{\mathbf{q},k\}$ is the 3D wave vector). Therefore, $D(q,t-t')$ has the following form

$$D(q,t-t') = -i\langle T[A_{\mathbf{q}}(t)A_{-\mathbf{q}}(t')]\rangle,$$

where

$$A_{\mathbf{q}} = \sum_k \eta_k \sum_{\mathbf{K}'} a^\dagger_{\mathbf{K}'-\mathbf{K}} a_{\mathbf{K}'}, \quad \eta_k = \langle 1|e^{ikz}|1\rangle,$$

T is the time-ordering operator, and $|1\rangle$ is the ground state of the SE's. Operators $A_{\mathbf{q}}$ depend on the electron state of the normal motion, since they represent a sort of projection of the 3D vapor atom system onto the plane of the 2D electron system. The form of $A_{\mathbf{q}}$ introduced above comes from the structure of the interaction Hamiltonian.

The perturbation procedure establishes the relation between the electron self-energy $\Sigma_N(E)$ and $G_N(E)$ in the frame, where the electron spectrum is discrete (for details see, for example, Ref. 23). In this frame, impurities move as a whole with the velocity $-\mathbf{u}_f$ and their Green's function is

affected by the Doppler shift $D(q,\omega+\mathbf{q}\cdot\mathbf{u}_f)\propto -in^{(a)}\delta(\omega+\mathbf{q}\cdot\mathbf{u}_f)$. After the integration over ω, the necessary relation can be written as

$$\Sigma_N(E)=\frac{1}{4}\Gamma_{se}^2\sum_{N'}\int_0^{2\pi}\frac{d\varphi}{2\pi}\int_0^{\infty}dx_q J_{N,N'}(x_q)\times G_{N'}(E+\hbar\mathbf{q}\cdot\mathbf{u}_f). \quad (4)$$

Here we use the following notations: Γ_{se} is the single-electron Landau level broadening, $x_q=q^2l^2/2$, and $J_{N,N'}(x_q)=|\langle N,X|\exp(-i\mathbf{q}\cdot\mathbf{r})|N',X-q_yl^2\rangle|^2$.

Equation (4) differs from the conventional SCBA result by the Doppler shift in the argument of the electron Green's function. If the energy exchange $\hbar\mathbf{q}\cdot\mathbf{u}_f\sim\Delta_f$ is much less than Γ_N, then we can disregard it, as well as the mixing of different Landau levels. In this limit, Eq. (4), together with the Dyson's equation for $G_N(E)$, yields the result of the SCBA: $\mathrm{Im}G_N(E)$ has a semielliptic shape with the Landau-level broadening $\Gamma_{se}=\hbar\sqrt{(2/\pi)\omega_c\nu_0}$, where ν_0 is the collision frequency at $B=0$.

In the general case, Eq. (4) is an integral equation and the level shape differs from the simple semi-elliptical function. Following Ref. 23, we simplify the problem by fixing the Landau-level shape to a Gaussian function (for example) and define $\Gamma_N\propto\mathrm{Im}\Sigma_N(E_N)$. This gives us the following equation:

$$\Gamma_N=\Gamma_{se}^2\sum_{N'}\frac{1}{\Gamma_{N'}}\int_0^{2\pi}\frac{d\varphi}{2\pi}\int_0^{\infty}dx_q J_{N,N'}(x_q)\times\exp\{-2[\hbar\omega_c(N'-N)-\sqrt{2x_q}\Delta_f\cos(\varphi)]^2/\Gamma_{N'}^2\}. \quad (5)$$

In Sec. II B, we will show that a more rigorous approach is in accordance with this result, proving the assumptions used here to be correct.

There are three important parameters appearing in Eq. (5):

$$\lambda=\frac{\Delta_f}{\Gamma_{se}},\quad \beta=\frac{\Gamma_{se}}{\hbar\omega_c},\quad \delta=\frac{\sqrt{2}\Delta_f}{\hbar\omega_c}. \quad (6)$$

The parameter λ is responsible for the suppression of electron scattering within a Landau level (term $N'=N$), when $\lambda\gtrsim 1$. The second parameter β describes the mixing of different Landau levels when Coulomb effects are disregarded. At $\Delta_f=0$, the mixing of sharp levels is very small due to $\beta\ll 1$. This parameter does not depend on the fluctuational electric field, though there is a weak dependence $\beta(n_s)$, due to the holding field dependence of the electron wave function and ν_0. The parameter δ (a combination of the parameters λ and β) is a measure of the stimulation of electron scattering between different Landau levels and mixing of Landau levels caused by the many-electron effect. For the mixing terms ($N'\neq N$), we can neglect Γ_N as compared to $\hbar\omega_c$. In this limit, the equation for the normalized Landau level broadening $g_N=\Gamma_N/\Gamma_{se}$ can be presented in the form

$$g_N^2=\chi_N(\lambda/g_N)+\frac{g_N}{2\lambda}C_N(\sqrt{2}\lambda\beta), \quad (7)$$

where

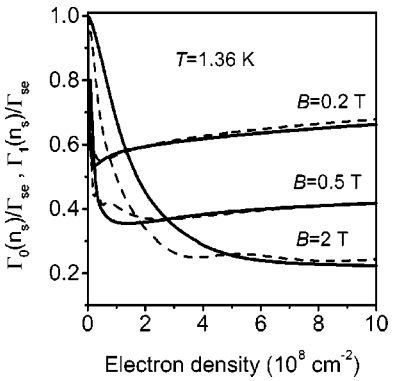

FIG. 1. The collision broadening of Landau levels [$N=0$ (solid curve) and $N=1$ (dashed curve)] vs n_s for three values of the magnetic field.

$$\chi_N(y)=\int_0^{\infty}dx[L_N(x)]^2e^{-(1+2y^2)x}I_0(2y^2x), \quad (8)$$

$I_0(z)$ is the Bessel function, and $L_N(z)$ is the Laguerre polynomial. In the most important cases $N=0$ and $N=1$, we can find

$$\chi_0(y)=\frac{1}{\sqrt{1+4y^2}},\quad \chi_1(y)=\frac{1+4y^2+12y^4}{(1+4y^2)^{5/2}}. \quad (9)$$

The general expression for $C_N(\delta)$ is rather complicated; therefore, we present equations for C_0 and C_1 only:

$$C_0(\delta)=\sum_{n=1}^{\infty}\frac{e^{-(n/\delta)^2}}{n!}\sum_{m=0}^{n}\frac{(2m-1)!!}{2^m}\left(\frac{n}{\delta}\right)^{2(n-m)}c_{n,m}, \quad (10)$$

$$C_1(\delta)=e^{1/\delta^2}\left(\frac{1}{\delta^2}+\frac{1}{2}\right)+\sum_{n=1}^{\infty}\frac{e^{-(n/\delta)^2}}{(n+1)!}\sum_{m=0}^{n}\frac{(2m-1)!!}{2^m}\times\left(\frac{n}{\delta}\right)^{2(n-m)}\left[\left(n+1-\frac{n^2}{\delta^2}-m-\frac{1}{2}\right)^2+m+\frac{1}{2}\right]c_{n,m}.$$

Here $c_{n,m}$ stands for the binomial coefficients ($c_{n,0}=1$). An analytical interpolation for $C_0(\delta)$ can be written as $C_0(\delta)\simeq(3\delta/\sqrt{\pi}-0.6+1/\delta^2)\exp(-1/\delta^2)$, which is valid for $0.4<\delta<5$ with an accuracy of 2%. It is clear that $C_0(\delta)$ is small for $\lambda\sim 1$, since $\delta\ll 1$ at $\beta\ll 1$. Still, it increases fast with λ and becomes important at $\delta\gtrsim 1$.

For the ground Landau level, the solution of Eq. (7) can be found in an analytical form, if we take into account that, at $\delta\sim 1$, the parameter $\lambda\gg 1$:

$$g_0^2(\lambda)=\sqrt{[1+C_0(\sqrt{2}\lambda\beta)]^2+4\lambda^4}-2\lambda^2. \quad (11)$$

For other Landau levels, Eq. (7) is solved numerically. The density dependence of the collision broadening of two Landau levels ($N=0$ and $N=1$) is shown in Fig. 1 for three values of B. The broadening decreases fast with n_s at low densities ($n_s<10^8$ cm^{-2}) and increases slowly (for $B<0.5$ T), or becomes nearly independent of n_s (for $B\gtrsim 0.5$ T) in the high-density range.

Thus the linewidth of the CR of SE's determined by $\langle\mathrm{Re}\sigma_{xx}(\omega)\rangle_f$ decreases with n_s in the low-density range, due

to the suppression of electron scattering within a Landau level (here $\langle\ \rangle_f$ means the average over the fluctuational field). The averaging over E_f makes the CR curve narrower in the vicinity of the peak and broader at the tails, with a rate depending on the strength of the many-electron effect $\Delta_f^{(0)}/\Gamma_{se}$, as if the Gaussian curve transforms into a Lorentzian one. It should be noted that in the low-density regime, the DK theory[17] predicts a shape that is noticeably different from a Lorentzian; still it also differs from a Gaussian, since this theory disregards the collision broadening of Landau levels.

Though the averaging over E_f changes the CR shape, the linewidth at the half height can be approximately described as

$$\hbar\gamma_G(n_s)\simeq\sqrt{\Gamma_0^2(n_s)+\Gamma_1^2(n_s)}/0.849. \tag{12}$$

According to this equation and Fig. 1, the CR linewidth has a finite value in the limit $\Delta_f\ll\Gamma_{se}$, and decreases fast in the low-density range, if $\Delta_f\gtrsim\Gamma_{se}$. In the high-density range, the dependence $\gamma_G(n_s)$ is a weak increase, due to mixing of different Landau levels. It should be noted that Eq. (3) cannot describe the effect of electron scattering between different Landau levels on the CR linewidth in the full extent. The strictest way to take into account these scattering processes is to consider the memory function approach.

B. Memory function formalism

Here we consider the memory function approach which allows one to incorporate the correlation effects in a more rigorous way. According to Refs. 2, 19, and 20, the conductivity tensor of 2D electrons can be expressed as

$$\sigma_{xx}\pm i\sigma_{xy}=\frac{ine^2/m}{\omega\mp\omega_c+M(\omega)}, \tag{13}$$

where $M(\omega)$ is the relaxation kernel. The real part of $M(\omega)$ determines the shift of the CR, while the imaginary part of $M(\omega)$ describes the CR linewidth. In our case, the shift of the CR is very small and, therefore, we confine our attention to $\mathrm{Im}\,M(\omega)$ which can be expressed in terms of the electron DSF,

$$\mathrm{Im}\,M(\omega)=(1-e^{-\hbar\omega/k_BT_e})\frac{\hbar^2\nu_0}{4m^2\omega}\sum_{\mathbf{q}}q^2S(q,\omega), \tag{14}$$

where

$$\nu_0=\frac{3U_a^2n^{(a)}\gamma_z m}{8\hbar^3}.$$

γ_z is the parameter of the electron wave function $\langle 1|z\rangle\propto z\exp(-\gamma_z z)$. Regarding the static conductivity $\sigma_{xx}(\omega=0)$, the expression for $\mathrm{Im}\,M(0)$ coincides with the expression for the effective collision frequency $\nu_{\mathrm{eff}}(B)$ of the extended SCBA,[24] which replaces ν_0 in the Drude conductivity equations. For the CR absorption, Eq. (13) results in a Lorentzian function with a frequency-dependent width parameter $\gamma_L(\omega)=2\mathrm{Im}\,M(\omega)$. In the ultraquantum limit, this parameter can be written as

$$\gamma_L(\omega)=\frac{\Gamma_{se}^2\omega_c}{4\hbar^2\omega}\int_0^\infty dx_q x_q S(q,\omega). \tag{15}$$

The most important thing is to find a proper approximation for the DSF $S(q,\omega)=N_e^{-1}\int e^{i\omega t}\langle n_{\mathbf{q}}(t)n_{-\mathbf{q}}(0)\rangle dt$, where $n_{\mathbf{q}}=\Sigma_e\exp(-i\mathbf{q}\cdot\mathbf{r}_e)$.

Let us first consider the *single-electron* approximation, which gives

$$S_{se}(q,\omega)=\frac{2\hbar}{\pi^2n_sl^2}\int dEf(E)[1-f(E+\hbar\omega)]$$
$$\times\sum_{N,N'}J_{N,N'}(x_q)\mathrm{Im}\,G_N(E)\mathrm{Im}\,G_{N'}(E+\hbar\omega).$$

Assuming $\hbar\omega_c\gg k_BT\gg\Gamma_{se}$, and $f\ll 1$, for the Gaussian level shape, one can find

$$S_{se}(q,\omega)=2\sqrt{\pi}\hbar\sum_{N=0}^{\infty}\frac{x_q^N}{N!\Gamma_{0,N}}$$
$$\times\exp[-x_q-\hbar^2(\omega-N\omega_c)^2/\Gamma_{0,N}^2]. \tag{16}$$

At $\omega\sim\omega_c$, the resonant term with $N=1$ dominates in Eq. (16), due to $\Gamma_N\ll\hbar\omega_c$. Then, according to Eq. (15), the frequency-dependent absorption width parameter of free electrons can be written as

$$\gamma_L(\omega)\simeq\frac{\sqrt{\pi}\Gamma_{se}^2\omega_c}{\Gamma_{0,1}\hbar\omega}\exp\left[-\frac{\hbar^2(\omega-\omega_c)^2}{\Gamma_{0,1}^2}\right]. \tag{17}$$

Here Γ_{se}^2 originates from ν_0 or from the electron-impurity interaction, while $\Gamma_{0,1}$ originates from the Landau-level broadening. For short-range scatterers, $\Gamma_N=\Gamma_{se}$ and $\Gamma_{0,1}=\Gamma_{se}$. It is interesting that according to Eq. (17), the frequency dependent width of the Lorentzian CR absorption function exhibits the resonant behavior itself which makes the CR line narrower in the region of tails [$\hbar(\omega-\omega_c)\sim\Gamma_{se}$]. For degenerate electrons, this effect was discussed in Ref. 19.

Physically, the frequency dependence of $\gamma_L(\omega)$ in Eq. (17) executes the transformation of the initial Lorentzian determined by Eq. (13) into the Gaussian CR curve of Eq. (3) which appears in the pure single-electron theory of Ando.[4] This transformation is shown in Fig. 2. The pure Gaussian function (solid curve) of the dimensionless variable x with the width parameter $w_G=0.08$ (the width at the half height $\gamma_G\simeq w_G/0.849$) and the pure Lorentzian function (dash-dotted curve) with the width at the half height $\gamma_L^{(0)}=\sqrt{\pi/2}w_G=\mathrm{const}$ give substantially different absorption curves, though their widths at the half-height are nearly the same. Conversely, the Lorentzian function with the frequency-dependent width defined according to Eq. (17), $\gamma_L(x)=\gamma_L^{(0)}\exp[-2(x-1)^2/w_G^2]$ (dashed curve), is quite close to the proper Gaussian function. We attribute the difference between the solid and dashed curves to the accuracy of the approximations used. For example, the frequency-dependent width model with $\gamma_L(x)=\gamma_L^{(0)}\exp[-2(x-1)^2/(\gamma_L^{(0)})^2]$ leads to a CR curve (dotted curve) which practically coincides with the Gaussian curve (solid curve). From Fig. 2 one can see

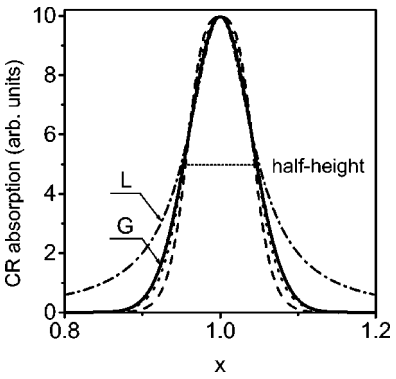

FIG. 2. Typical CR absorption curves: Gaussian (solid), Lorentzian (dash-dotted), frequency-dependent width models (dashed and dotted) presented according to the memory function formalism as described in the text.

that both approaches [the Ando theory (solid curve) and the memory function formalism (dashed curve)] give nearly the same CR absorption curves, if the Coulomb interaction between electrons is neglected.

From Eq. (17) and the density dependence of $\Gamma_{0,1}(n_s)$ established in Sec. II A, it might be concluded that the Coulomb effect should start with a broadening of the CR linewidth [$\gamma_L(\omega_c) \propto 1/\Gamma_{0,1}(n_s)$], which would be opposite to the result of Eq. (12). The explanation of this paradox is based on the fact that the single-electron approximation for the DSF of Eq. (16) is not appropriate for electrons with ultrafast orbit centers.

The *many-electron* DSF of electrons with ultrafast orbit centers can be found in the following way. Since the many-electron fluctuational field can be considered as a quasiuniform one, the problem of strongly interacting electrons reduces to the problem of independent electrons with ultrafast drift velocities $\mathbf{u}_f$ distributed accordingly. We can describe the system as an ensemble of independent electrons; each of them has its own drift velocity $\mathbf{u}_f^{(i)}$with regard to the electron liquid center-of-mass frame. The time averaging is substituted by the averaging over the ensemble. The contribution of one electron to the electron liquid DSF has the form of Eq. (16) in the local frame, moving along with the electron orbit center. When changing the reference frame, the DSF has the transcription rule $S'(q,\omega)=S(q,\omega-\mathbf{q}\cdot\mathbf{u})$. Therefore, in the electron-liquid center-of-mass frame, the DSF of an electron can be written as $S_{\rm se}(q,\omega-\mathbf{q}\cdot\mathbf{u}_f)$, and the proper many-electron approximation for the DSF of the ensemble of independent electrons exposed to the fluctuational field can be found as $S_{\rm me}(q,\omega)=\langle S_{\rm se}(q,\omega-\mathbf{q}\cdot\mathbf{u}_f)\rangle_f$. For the Gaussian distribution of E_f, we have

$$S_{\rm me}(q,\omega)=\int_0^\infty dy e^{-y}\int_0^{2\pi}\frac{d\varphi}{2\pi} \times S_{\rm se}[q,\omega-\sqrt{2x_q y}\cos(\varphi)\Delta_f^{(0)}/\hbar], \quad (18)$$

where y represents the ratio $(E_f/E_f^{(0)})^2$, and φ is the angle between the drift velocity $\mathbf{u}_f$ and the momentum exchange $\hbar\mathbf{q}$. We use the superscript (0) for the parameters Δ_f, λ, and δ taken at $E_f=E_f^{(0)}$.

It is very instructive to analyze the case when the dependence $\Gamma_N(E_f)$ is weak enough to be disregarded in the integral of Eq. (18) with $S_{\rm se}$ from Eq. (16). Strictly, this assumption is valid for rather high electron densities, according to Fig. 1. Still it is possible to prove that the integral of Eq. (18) is organized in such a way that the final result depends weakly on the real behavior of $\Gamma_N(E_f)$ in the whole density range. In this case, replacing $\Gamma_N(E_f)$ by $\Gamma_N(E_f^{(0)})$, and averaging over the fluctuational field, Eq. (18) can be transformed as

$$S_{\rm me}(q,\omega)=2\sqrt{\pi}\hbar\sum_{N=0}^{\infty}\frac{x_q^N}{N!\sqrt{\Gamma_{0,N}^2+2x_q(\Delta_f^{(0)})^2}} \times\exp\left[-x_q-\frac{\hbar^2(\omega-N\omega_c)^2}{\Gamma_{0,N}^2+2x_q(\Delta_f^{(0)})^2}\right]. \quad (19)$$

Like the DSF of noninteracting electrons [Eq. (16)], the many-electron DSF of Eq. (19) is a sum of Gaussian terms exhibiting resonant behavior with regard to $\omega-N\omega_c$ (with $N=0,1,2,\ldots$). The important difference is that $\Gamma_{0,N}$ is replaced by $\Gamma_{0,N}^{(*)}(q)=\sqrt{\Gamma_{0,N}^2(E_f^{(0)})+2x_q(\Delta_f^{(0)})^2}$. Thus the many-electron effect, that narrows Landau levels in the frame moving along with the electron orbit center, broadens the electron DSF in the electron liquid center-of-mass frame. Moreover, the rule of combining the collision broadening and the many-electron effect resembles the rule of combining the contributions of two different scattering mechanisms.[23]

One can see that $\Gamma_{0,1}^{(*)}(q)$ increases with n_s in spite of the decrease of $\Gamma_{0,1}(n_s)$, which is the solution of the above-mentioned paradox: the most important resonant term ($N=1$) of Eq. (19) decreases with n_s, causing the a decrease of the CR linewidth $\gamma_L(\omega_c)\propto 1/\Gamma_{0,1}^{(*)}(q)$. The many-electron effect broadens all terms of Eq. (19), and at high enough densities the contribution of nonresonant terms ($N\neq 1$) become important, if $\sqrt{2}\Delta_f^{(0)}\gtrsim\hbar\omega_c$. This is the origin of the Coulomb broadening of the CR at high electron densities.

Before proceeding with the CR absorption, we perform some checks. It is obvious that, in the limiting case $\Delta_f\to 0$, Eq. (19) reproduces the result of the SCBA for the electron DSF. In the opposite limiting case $\Gamma_{0,N}\ll 2\Delta_f^{(0)}$and $\omega\to 0$, Eq. (19) reproduces the results of the DK theory for the DSF and for the static magnetoconductivity.[16] The dc magnetoconductivity of electrons $\sigma_{xx}(0)$ is described by the first term of Eq. (19) with $N=0$. In this case, the many-electron effect acts on the electron DSF of the center-of-mass frame as an effective increase of the Landau-level broadening $\Gamma_0\to\Gamma_0^{(*)}(q)=\sqrt{\Gamma_0^2+2x_q(\Delta_f^{(0)})^2}$, though the real broadening Γ_0 determined in the frame moving along with the electron orbit center decreases with $\Delta_f^{(0)}$.[21]

For microwave radiation frequencies $\omega\sim\omega_c$ used in CR studies, at low electron densities, the main contribution to Eq. (19) comes from the resonant term ($N=1$), due to $\Gamma_N\ll\hbar\omega_c$. The nonresonant terms ($N\neq 1$) become important only at $\delta^{(0)}\gtrsim 1$. When describing the nonresonant terms, we can put $\omega=\omega_c$, since their contribution to $\gamma_L(\omega)$ is practically independent of small $\omega-\omega_c$. Thus we can write the frequency-dependent width as a sum of resonant ($N=1$) and nonresonant terms:

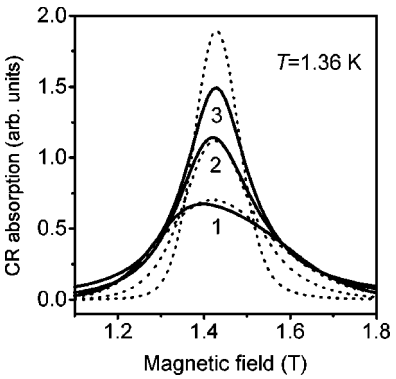

FIG. 3. The CR line-shape transformation caused by the many-electron effect: the memory function formalism, according to Eqs. (20)–(22) (solid curves), and the density-dependent Landau level width approach described in Sec. II A (dashed curves). Electron density $n_s=0.3\times10^8$ cm^{-2} (1), 1.0×10^8 cm^{-2} (2), and 5.0×10^8 cm^{-2} (3).

$$\gamma_L(\omega)=\gamma_L^{(R)}(\omega)+\gamma_L^{(\mathrm{NR})}, \tag{20}$$

where

$$\gamma_L^{(R)}(\omega)=\frac{\sqrt{\pi}\Gamma_{\mathrm{se}}^2\omega_c}{2\hbar\omega}\int_0^\infty\frac{x^2\exp(-x)}{\sqrt{\Gamma_{0,1}^2+2x(\Delta_f^{(0)})^2}}\times\exp\left[-\frac{\hbar^2(\omega-\omega_c)^2}{\Gamma_{0,1}^2+2x(\Delta_f^{(0)})^2}\right]dx, \tag{21}$$

$$\gamma_L^{(\mathrm{NR})}=\frac{\sqrt{\pi}\Gamma_{\mathrm{se}}}{2\hbar}\frac{\Gamma_{\mathrm{se}}}{\hbar\omega_c}A(\delta^{(0)}), \tag{22}$$

$$A(\delta)=2\sum_{N(\neq1)}\frac{|N-1|^{N+3/2}}{N!\,\delta^{N+5/2}}K_{N+3/2}(2|N-1|/\delta).$$

$K_\nu(z)$ is the Bessel function, and $\delta^{(0)}=\sqrt{2}\Delta_f^{(0)}/\hbar\omega_c$. For simple estimations of the effect of stimulation of electron scattering between Landau levels, one can use the interpolation formula $A(\delta)\simeq3.2\delta^{0.94}\exp[-(0.3/\delta)^3]$, which is approximately valid at $\delta\leqslant1.1$.

According to Eqs. (20)–(22), the CR line shape changes in the following way. The resonant term $\gamma_L^{(R)}(\omega)$, which makes a Gaussian from the initial Lorentzian function in the single-electron theory, as shown in Fig. 2, becomes more and more broadened with the electron-density increase due to the Coulomb correction $\sqrt{2x_q}\Delta_f^{(0)}$. Qualitatively, this effect can be described by Eq. (17), where $\Gamma_{0,1}$ should be replaced by $\sqrt{\Gamma_{0,1}^2+2(\Delta_f^{(0)})^2}$, according to Eq. (21) and the estimation $x_q\sim1$. This additional broadening of the resonant term $\gamma_L^{(R)}$ reduces its amplitude $\gamma_L^{(R)}(\omega_c)$ and narrows the CR linewidth. When $\sqrt{2}\Delta_f^{(0)}$ increases above $\Gamma_{0,1}$, the width function $\gamma_L(\omega)$ becomes less and less dependent of ω within the CR resonance frequency range $\omega-\omega_c\lesssim\Gamma_{0,1}$, which transforms the Gaussian absorption curve of noninteracting electrons into a Lorentzian curve of electrons with ultrafast orbit centers. In the limiting case $\sqrt{2}\Delta_f^{(0)}\gg\Gamma_{0,1}$, the CR line shape becomes a pure Lorentzian function.

The transformation of the CR line shape caused by the many-electron effect is shown in Fig. 3 for three electron densities. At two lowest densities the curves calculated according to Eqs. (20)–(22) (solid curve) and according to the density-dependent Landau-level width model described in Sec. II A (dashed curve) are quite close. The small asymmetry of the first solid curve is probably caused by the breakdown of the approximation $\Gamma_N\ll k_BT$. For the highest density of Fig. 3, the difference between these two approaches become large, due to the effect of stimulation of electron scattering between different Landau levels.

According to Fig. 2, the width at the half-height of the Lorentzian function with the frequency-dependent width parameter $\gamma=\gamma_L(\omega)$ is practically the same as the width of the conventional Lorentzian with $\gamma=\gamma_L(\omega_c)$. The latter quantity can be evaluated without the assumption $\Gamma_N\simeq\Gamma_N(E_f^{(0)})$ in the resonant term $(N=1)$. Direct evaluation of the resonant term $\gamma_L^{(R)}(\omega_c)$ based on Eqs. (14) and (18) gives

$$\gamma_L^{(R)}(\omega_c)=\frac{\sqrt{\pi}\Gamma_{\mathrm{se}}}{2\hbar}\int_0^\infty e^{-y}W_{0,1}(\lambda^{(0)}\sqrt{y})dy, \tag{23}$$

where

$$W_{0,1}(\lambda)=\frac{3(g_{0,1}^2+\lambda^2)^2}{(g_{0,1}^2+2\lambda^2)^{5/2}}-\frac{g_{0,1}^2}{(g_{0,1}^2+2\lambda^2)^{3/2}};$$

and $g_{0,1}=\Gamma_{0,1}/\Gamma_{\mathrm{se}}\equiv\sqrt{(g_0^2+g_1^2)/2}$ is the function of λ, according to Eq. (7). The nonresonant term $\gamma_L^{(NR)}$ remains the same as in Eq. (22).

In the extreme many-electron limit $(\Delta_f^{(0)}\gg\Gamma_{\mathrm{se}})$, neglecting $\gamma_L^{(\mathrm{NR})}(\omega_c)$, Eq. (23) reproduces the result of the DK theory which, we represent as

$$\gamma_L(\omega_c)\approx\frac{3\pi}{8\sqrt{2}}\frac{\Gamma_{\mathrm{se}}^2}{\hbar\Delta_f^{(0)}}\propto\frac{1}{n_s^{3/4}}. \tag{24}$$

The approximation of the ultrafast electron orbit centers introduced here restricts this result from both low- and high-electron-density ranges. In the low-density limit $(\Delta_f^{(0)}\ll\Gamma_{\mathrm{se}})$, $\gamma_L(\omega_c)\sim\Gamma_{\mathrm{se}}/\hbar$ is practically independent of n_s. In the high-density range $(\Delta_f^{(0)}\gtrsim\hbar\omega_c)$, the nonresonant term $\gamma_L^{(\mathrm{NR})}$ becomes important, increasing $\gamma_L(\omega_c)$ and changing the sign of the many-electron effect, due to electron scattering between different Landau levels.

In the general case, we evaluated Eqs. (22) and (23) numerically. The results for $\gamma_L(\omega_c)$ are shown in Fig. 4 as solid curves found for three values of B. The corresponding results of the previously described density-dependent Landau-level width model [γ_G of Eq. (12)] are shown as dashed curves. Though the curves of the weakest magnetic field ($B=0.2$ T) do not correspond the conditions of the quantum CR of the electron-vapor atom-scattering regime, we will show that they explain qualitatively the experimental results of Ref. 18 found for the electron-ripplon scattering regime. The electron density range which corresponds to the range of parameter λ of Fig. 4 is different for each solid curve, due to the field dependence of $\Gamma_{\mathrm{se}}(B)\propto\sqrt{B}$ and $\Delta_f(B)\propto1/\sqrt{B}$ [or $\lambda(B)\propto1/B$]. Thus, for $B=0.2$ T, the range $\lambda<5$ is realized for $n_s<0.72\times10^8$ cm^{-2}, while for $B=3$ T the corresponding density range is substantially wider: $n_s<37\times10^8$ cm^{-2}.

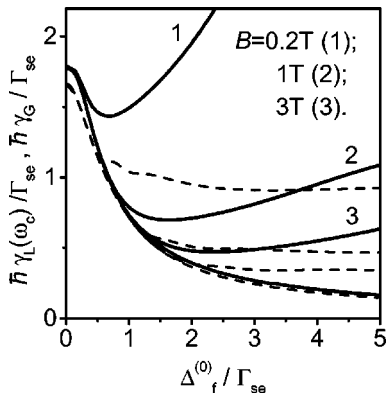

FIG. 4. The CR linewidth vs the many-electron parameter $\lambda^{(0)} = \Delta_f^{(0)}/\Gamma_{se}$ at $T = 1.36$ K for three typical resonant magnetic fields: the memory function formalism (solid curves) and the density-dependent Landau-level width approach (dashed curves). The lowest curves (solid and dashed) are plotted for the limiting case $\hbar\omega_c \gg \Delta_f^{(0)}$.

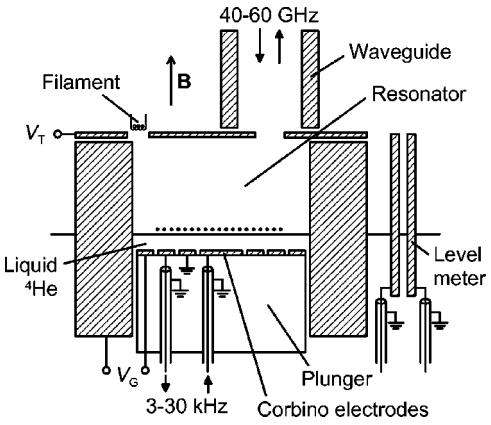

FIG. 5. Schematic diagram of the experimental cell.

It is instructive to compare the resonant term of Eq. (23) (the lowest solid curve of Fig. 4), describing the effect of suppression of electron scattering, with Eq. (12) of the alternative approach for γ_G (the lowest dashed curve), neglecting the effect of mixing of Landau levels. These curves correspond to the limiting case $\hbar\omega_c \gg \Delta_f^{(0)}$. One can see that the approach based on the memory function formalism and the density-dependent Landau-level width approach give remarkably very close curves. The small relative increase of the solid curve in the limit $\lambda_f^{(0)} \to 0$ reflects the shaping effect: in this range the CR shape of the memory function approach is not a Lorentzian function, but a function which is close to a Gaussian with the width at half-height equal $\sqrt{2/\pi}\gamma_L/0.849 \simeq 0.94\gamma_L$. There is no doubt that both theoretical approaches result in the same Coulomb narrowing effect on the CR linewidth.

Contrary to the Coulomb narrowing, the broadening of the CR induced by the many-electron effect is described differently by each of the two approaches introduced above. The increase of the CR linewidth with n_s is substantially stronger for the memory function formalism, as shown in Fig. 4 for three values of the magnetic fields ($B = 0.2$ T, 1 T, and 3 T) (solid curves 1, 2, and 3). One can see that the weak increase of the broadening of Landau levels due to the mixing effect (dashed curves) cannot be a measure of the many-electron broadening of the CR. This is reasonable, because the probability of electron scattering between different Landau levels induced by the high-energy exchange $\Delta_f^{(0)} \gtrsim \hbar\omega_c$ does not actually depend on the Landau-level broadening for $\Gamma_N \ll \hbar\omega_c$. Additionally, the presentation of Fig. 4 shows that the magnetic-field dependence of the Coulomb narrowing can be normalized by $\Gamma_{se} \propto \sqrt{B}$, while the Coulomb broadening still decreases with B, approaching the lowest solid curve, since the Landau-level separation $\hbar\omega_c \propto B$ increases faster with B than Γ_{se}.

Figure 4 shows also that the many-electron effect changes its sign at a rather small value of the parameter $\Delta_f^{(0)}/\hbar\omega_c$ due to the fast decrease of the resonant term $\gamma_L^{(R)}$ with $\lambda^{(0)}$. This means that the CR narrowing and most of the CR broadening of Fig. 4 occurs at conditions where the fluctuational electric field can be considered as quasiuniform. Beyond this regime, our approach takes into account only the uniform part of the fluctuational field which induces drift velocities $\mathbf{u}_f^{(i)}$. Since the main effect described here originates from the ultrafast fluctuational motion of electron orbit centers, we may assume that our approach will be qualitatively valid even for nonuniform fluctuational fields.

III. EXPERIMENT

The main experimental difficulty in observing Coulomb narrowing of the CR linewidth for SE's on the free surface of liquid helium, as can be seen from Figs. 1 and 4, lies in the fact that it requires a combination of a strong resonant magnetic field [or a high frequency of the microwave (MW) radiation] together with the possibility of measuring down to very low electron densities. This implies a high sensitivity of the detection system used.

For our measurements, we use a MW spectrometer working at frequencies of 40–60 GHz. Figure 5 shows a schematic view of the low-temperature part of the setup. It consists essentially of a metallic cavity in the form of an upright cylinder, acting as a resonator for microwaves in the TE_{011} mode. The bottom plate of the cavity is mounted on a movable plunger to enable the height of the resonator to be changed, and thus to tune its resonance frequency *in situ*. The cavity has a diameter of 10.8 mm and a height between 7 mm (at 40 GHz) and 3 mm (at 60 GHz). The resonator is operated in reflection mode through a single rectangular waveguide, ending above a coupling hole in the top plate. For signal detection, a phase-sensitive heterodyne system with high sensitivity is employed. To avoid possible lineshape distortions due to a heating of the electron system, the MW input power is kept at an estimated level of below 10^{-18} W per electron. At this level the line shape is in the equilibrium regime, as we verified in a former study of the power dependence of the CR.[15] For further details of the microwave part of the setup, we refer to Ref. 25.

Top and bottom plates as well as the sidewall of the cavity are electrically isolated from each other, and can be put at different potentials. Furthermore, the bottom plate consists of an array of four concentric electrodes in Corbino configuration. Of these, the central one and the third are used to measure the complex conductance of the electron layer at low

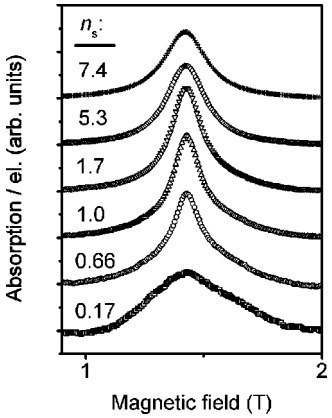

FIG. 6. The CR absorption data at $T=1.36$ K for six electron densities shown in units 10^8 cm^{-2}.

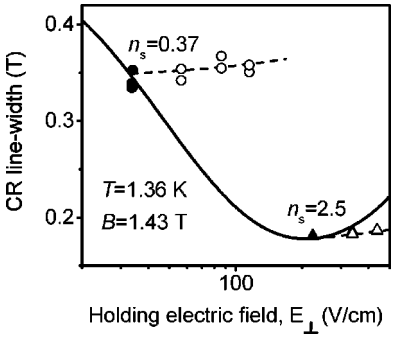

FIG. 7. The CR linewidth data vs $E_\perp$ for fixed electron densities: $n_s \simeq 0.37\times 10^8$ cm^{-2} (circles) and $n_s \simeq 2.5\times 10^8$ cm^{-2} (triangles); solid symbols represent the saturation condition $E_\perp = 2\pi e n_s$. The CR linewidth is given by the memory function formalism [Eqs. (20)–(22)]. The saturation condition is shown by the solid curve, and the fixed electron density conditions by the dashed curves.

frequencies between 3 and 30 kHz in order to check whether we have conventional results for the Coulomb effect on the static magnetoconductivity $\sigma_{xx}(0)$,[26] as described in Ref. 21, while the second electrode is put at ground to reduce the direct cross-talk between the measuring electrodes. The fourth and most outward electrode is usually put on the same negative potential V_G as the side wall of the cavity and the two act together as guard electrodes.

In the experiment, the cavity is partly filled with liquid helium to a height of typically 0.6 mm above the bottom plate. Electrons are produced by heating a small filament placed in a hole in the top plate, and confined to the helium surface by negative potentials applied to the top plate and guard electrodes, while the Corbino electrodes correspond to the ground potential.

Most of the CR measurements presented here were performed with varying electron densities n_s under the saturation condition $2\pi e n_s = E_\perp$, when the electric field of the electron layer screens completely the external electric field $E_\perp$ above the layer. In these measurements, the voltages applied to the top plate and guard electrodes were kept the same $V_T = V_G$, and, after the procedure described in Ref. 27, we used the capacitance measured across the Corbino electrodes to ensure that the electron density always corresponded to saturation. Since the electron-vapor atom interaction is nearly independent of the holding field $E_\perp$, especially at low electron densities, the density dependence of the linewidth observed in our experiments reflects the many-electron effect produced by the fluctuational electric field E_f.

The raw CR absorption data are shown in Fig. 6 for six typical electron densities. The absorption line of the lowest density is substantially broader than the others, and its shape can be nicely fitted with a Gaussian function. On the other hand, the absorption lines of high enough densities ($n_s \geqslant 1.7\times 10^8$ cm^{-2}) have pure Lorentzian shapes. The CR line shape of the intermediate densities is a sort of mixture of Gaussian and Lorentzian. Figure 6 shows the successive narrowing and broadening of the CR linewidth with the increase of electron density.

To check that the observed phenomena are caused solely by many-electron effects, we performed some measurements at a fixed electron density, varying only the holding electric field $E_\perp$ (i.e., at nonsaturated conditions). In this case, also according to the procedure described in Ref. 27, the top plate voltage V_T determined the value of the pressing electric field, while the voltage applied to the guard electrodes V_G was adjusted accordingly to keep the electron density always at a constant value. We chose two distinctive densities: one in the low density regime ($n_s \simeq 0.37\times 10^8$ cm^{-2}), and another one in the vicinity of the minimum of the CR linewidth ($n_s \simeq 2.5\times 10^8$ cm^{-2}). The corresponding data are shown in Fig. 7, together with theoretical curves calculated according to Eqs. (22) and (23). The most important conclusion which follows from this figure is that the holding field dependence is much weaker than the density dependence (solid curve) of the CR linewidth, even for the Coulomb broadening regime. Another important point is that an increase of $E_\perp$ may cause only an increase of the CR linewidth due to the field dependence of the electron localization length $\gamma_z^{-1}(E_\perp)$ in the perpendicular direction. This weak dependence is in accordance with the theoretical curves (dashed) shown in Fig. 7. An increase of $E_\perp$ even qualitatively cannot be an origin for the Coulomb narrowing of the CR, and the latter represents a pure many-electron effect.

IV. EXPERIMENT-THEORY COMPARISON AND DISCUSSIONS

Before proceeding with the analysis of our data, we consider the conditions of the experiment,[18] where there was no sign of the Coulomb narrowing of the CR linewidth observed, in contradiction with the DK theory.[16] In that paper, the linewidth data had shown a linear increase with n_s in the range: 0.2×10^8 cm$^{-2} \lesssim n_s < 4.5\times 10^8$ cm^{-2}. The temperature of the system was quite low ($T=0.062$ K), which means that the electron-ripplon scattering dominated the electron transport and the electron system was mostly in the Wigner solid state (though the onset of electron crystallization was not observed with CR). The important point is that the magnetic field used in Ref. 18 was very weak (less than 0.1 T). Under these conditions, the additional energy exchange caused by the ultrafast orbit centers $\Delta_f^{(0)}$ is larger than the Landau-level separation $\hbar\omega_c$ in the whole range of electron densities used there. This correction does not depend on the kind of scatterers present, and is surely applicable for electron-ripplon scattering in the moving frames. This means

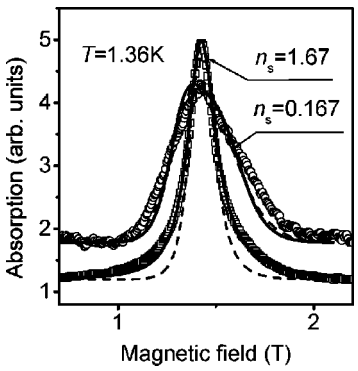

FIG. 8. The CR absorption for two electron densities (circles and squares). The memory function formalism is shown by the solid curves, and the density-dependent Landau-level width approach by the dashed curves.

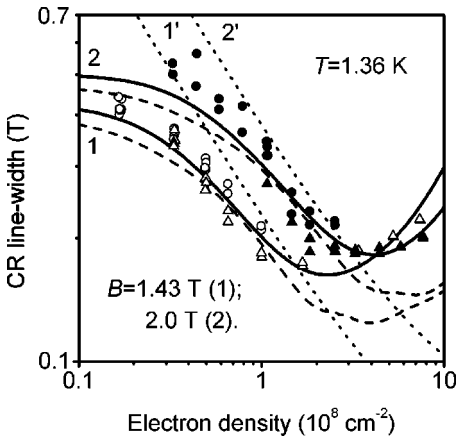

FIG. 9. The CR linewidth vs n_s for two resonant values of B: $B=1.43$ T (symbols of open style) and $B=2.0$ T (symbols of solid style). Also given are the Gaussian fitting data (circles), the Lorentzian fitting data (triangles), the memory function formalism according to Eqs. (22) and (23) (solid curves), the density-dependent Landau-level width approach (dashed curves), and the theory of Dykman and Khazan (dotted curves).

that electron scattering between different Landau levels dominated the CR linewidth. In this case, the main contribution to $\gamma_L(\omega_c)$ comes from the nonresonant terms $[\gamma_L^{(\mathrm{NR})} \gg \gamma_L^{(R)}(\omega_c)]$ increasing with n_s. Qualitatively this effect is seen in Fig. 4, where the highest curve is plotted for $B=0.2$ T. The reduction of the CR linewidth is very small and occurs at very low electron densities $n_s \lesssim 5\times 10^6$ cm^{-2}, which is far beyond the density range used in Ref. 18. Moreover, in the density range used in this experiment, the theory based on the memory function formalism presented here gives approximately linear increase of the CR linewidth with n_s, which is in accordance with the data reported.

Regarding our data, we apply substantially stronger magnetic fields, which places the minimum of the theoretical curves in the middle of the electron-density range used. Comparing the data with the theoretical concept, we check first whether the presented theory can describe the transformation of the CR line shape observed with the increase of electron density. As we already mentioned, the qualitative accordance with the theory is obvious: it follows from Fig. 6. The lowest density data can be nicely fitted by a Gaussian, while the medium- and high-density data follow a Lorentzian absorption curve. The shape transformation starts as a narrowing of the absorption curve in the vicinity of the resonance $\omega \sim \omega_c$, leaving the tails unchanged, which is also in accordance with the theoretical curves of Fig. 3. To compare the data and the theory quantitatively, in Fig. 8 we show two typical data plots and corresponding theoretical curves calculated according to Eqs. (20)–(22). For a comparison, we also show the result of the density-dependent Landau-level width model (dashed curves). For the lowest electron density, the data plot has a slightly wider linewidth than the theoretical curve, while for the higher density the solid theoretical curve perfectly fits the CR data with no adjusting parameter.

The CR linewidth at half height of the experimental data is found here by fitting the absorption data to the conventional Gaussian or Lorentzian functions. As the CR absorption line is generally a sort of mixture of Lorentzian and Gaussian, there is a small difference between these two fitting sets of data. Since at low electron densities, the line shape is mostly a Gaussian and at higher densities ($n_s \geqslant 1.7\times 10^8$ cm^{-2}) it is a Lorentzian, we present the Gaussian fitting linewidth data (circles) for low and medium n_s and the Lorentzian fitting data (triangles) for medium and high n_s. These two sets of data overlap in the range of medium electron densities, as shown in Fig. 9 for two values of the resonant magnetic field. In this figure, the theory presented here (solid curves 1 and 2) contains no adjusting parameter. The possible contribution from the electron-ripplon interaction is very small in the density range shown in the figure. For Landau-level broadening it varies from 0.7% (lowest density) to 12% (highest density). In Fig. 9, we took it into account as an appropriate increase of Γ_{se} calculated according to the results of Refs. 12 and 23 for electron-ripplon scattering.

According to Fig. 9, the increase of the resonant frequency ω as compared to the condition of Ref. 15 shifts the Coulomb narrowing into the range of higher electron densities. This is caused by an increase of the Landau-level broadening with the magnetic field $\Gamma_{se} \propto \sqrt{B}$. This is also valid for the results of the DK theory shown in this figure as dotted curves. The theory presented here (solid curves) and the density-dependent Landau-level width model (dashed curves) both deviate from the DK theory in the range of low electron densities in the same way, and describe the CR linewidth data much better. In the range of high electron densities the experimental data and the solid curves also deviate strongly from the dotted curves, and the increase of the CR linewidth with n_s is nicely described by our theory. Both the two solid theoretical curves and the two data plots of different resonant frequencies cross at high n_s practically in the same point. This means that the increase of the magnetic field suppresses the broadening of the CR, making the effect of Coulomb narrowing stronger in accordance with the theoretical concept of stimulation of electron scattering between different Landau levels.

It is very instructive to use the presentation of Fig. 4, normalizing the CR linewidth by Γ_{se}, for the experimental data as well. In this case, we use values of Γ_{se} calculated for each experimental density and magnetic field according to the SCBA theory for the electron-vapor atom interaction. The result of this normalization is shown in Fig. 10. Contrary

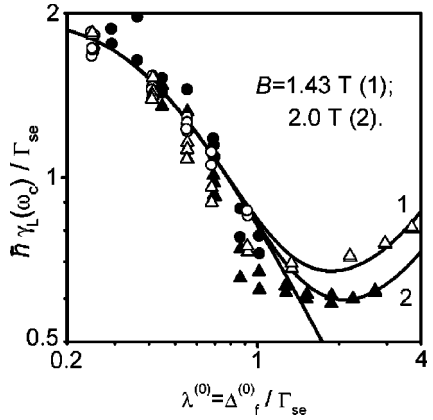

FIG. 10. The normalized CR linewidth data and the theory vs $\lambda^{(0)}=\Delta_f^{(0)}/\Gamma_{se}$ for two resonant frequencies. Notations are the same as in Fig. 9.

to Fig. 9, here we disregard electron-ripplon interaction, and to adjust the theory to the data all the theoretical curves are shifted slightly up by 11%. One can see that the effect of the magnetic field on the Coulomb narrowing of the CR is perfectly normalized by $\Gamma_{se}\propto\sqrt{B}$. Conversely, the Coulomb broadening of the CR with n_s cannot be normalized in such way, since this effect is described by the parameter $\delta^{(0)}=\sqrt{2}\Delta_f^{(0)}/\hbar\omega_c$ rather than by $\lambda^{(0)}=\Delta_f^{(0)}/\Gamma_{se}$. For the experimental data ($B=1.43$ T) of Fig. 10, the parameter $\Delta_f^{(0)}/\hbar\omega_c$ varies in the range $0.04<\Delta_f^{(0)}/\hbar\omega_c<0.7$. It should be noted that the accuracy of determination of the CR linewidth from the absorption data increases with electron density because for higher densities we have a stronger signal.

V. CONCLUSIONS

We have investigated the influence of strong internal forces on the CR absorption from a 2D electron system with extremely narrow Landau levels. In the presence of a strong magnetic field, the fluctuational internal electric fields are quasiuniform, and the system can be considered as an ensemble of nearly independent electrons whose orbit centers are moving ultrafast with the drift velocity distributed according to the distribution of the fluctuational field. The transcription into local frames moving along with each orbit center eliminates the fluctuational field, restores the Landau spectrum, and makes electron scattering substantially inelastic due to the Doppler shift $\hbar\mathbf{q}\cdot\mathbf{u}_f$. Two theoretical models have been analyzed: (1) the model of independent electrons based on the Ando CR theory[4] and on the inelastic SCBA, with the Landau-level broadening Γ_N affected by the ultrafast drift velocity $\mathbf{u}_f$;[15] and (2) the memory function formalism[19,20] with our approximation for the electron dynamic structure factor, taking into account the ultrafast motion of electron orbit centers. For low and medium electron densities, both theoretical models result in practically the same Coulomb narrowing of the CR linewidth due to the inelastic suppression of electron scattering within the ground Landau level. For high electron densities, when the ultrafast drift velocities of electron orbits stimulate electron scattering between different Landau levels, the memory function formalism results in the Coulomb broadening of the CR which is much stronger than the increase of the collision broadening of Landau levels.

Experimental studies of the CR absorption from the 2D electron system formed on the free surface of superfluid helium reported here have shown this strong successive narrowing and broadening of the CR linewidth with the increase of electron density. All the tests performed in studying these many-electron effects appeared to be in accordance (even numerical) with the theoretical concept presented. The density dependence of the CR linewidth found for two resonant frequencies and the transformation of the line shape caused by the many-electron effect are nicely described by the memory function approach reported above. Even the different response of the Coulomb narrowing and broadening to an increase of the resonant frequency observed is in accordance with the theoretical model, describing the many-electron effects as suppression and stimulation of electron scattering caused by the ultrafast motion of electron orbit centers. Our studies eliminate the conflict between experiment and theory reported in Ref. 18 and might give a new explanation for the many-electron narrowing of the CR reported long ago for semiconductor 2D electron systems.

ACKNOWLEDGMENT

A part of this work was supported by an INTAS-97-1643 grant.

[1] T. Ando, A. B. Fowler, and F. Stern, Rev. Mod. Phys. **54**, 437 (1981).
[2] C. S. Ting, S. C. Ying, and J. J. Quinn, Phys. Rev. B **16**, 5394 (1977).
[3] T. Ando and Y. Uemura, J. Phys. Soc. Jpn. **36**, 959 (1974).
[4] T. Ando, J. Phys. Soc. Jpn. **38**, 989 (1975).
[5] T. A. Kennedy, R. J. Wagner, B. D. McCombe, and D. C. Tsui, Solid State Commun. **22**, 459 (1977).
[6] B. A. Wilson, S. J. Allen, Jr., and D. C. Tsui, Phys. Rev. Lett. **44**, 479 (1980).
[7] B. A. Wilson, S. J. Allen, Jr., and D. C. Tsui, Phys. Rev. B **24**, 5887 (1981).
[8] Y. Shiwa and A. Isihara, Solid State Commun. **53**, 519 (1985).
[9] Z. Schlesinger, W. I. Wang, and A. H. MacDonald, Phys. Rev. Lett. **58**, 73 (1987).
[10] C. Kallin and B. I. Halperin, Phys. Rev. B **31**, 3635 (1985).
[11] *Two-Dimensional Electron Systems on Helium and other Substrates*, edited by E. Andrei (Kluwer, New York, 1997).
[12] Yu. P. Monarkha, S. Ito, K. Shirahama, and K. Kono, Phys. Rev. Lett. **78**, 2445 (1997).
[13] T. R. Brown and C. C. Grimes, Phys. Rev. Lett. **29**, 1233 (1972).
[14] V. S. Edel'man, Zh. Éksp. Teor. Fiz. **77**, 673 (1979) [Sov. Phys. JETP **50**, 338 (1979)].
[15] E. Teske, Yu. P. Monarkha, M. Seck, and P. Wyder, Phys. Rev. Lett. **82**, 2772 (1999).
[16] M. I. Dykman and L. S. Khazan, Zh. Éksp. Teor. Fiz. **77**, 1488

(1979) [Sov. Phys. JETP **50**, 747 (1979)].
[17] M. I. Dykman, C. Fang-Yen, and M. J. Lea, Phys. Rev. B **55**, 16 249 (1997).
[18] L. Wilen and R. Giannetta, Phys. Rev. Lett. **60**, 231 (1988).
[19] W. Gotze and J. Hajdu, Solid State Commun. **29**, 89 (1979).
[20] Y. Shiwa and A. Isihara, J. Phys. C **16**, 4853 (1983).
[21] Yu. P. Monarkha, E. Teske, and P. Wyder, Phys. Rev. B **59**, 14 884 (1999).
[22] R. R. Gerhardts, Surf. Sci. **58**, 227 (1976).
[23] Yu. P. Monarkha, K. Shirahama, K. Kono, and F. M. Peeters, Phys. Rev. B **58**, 3762 (1998).
[24] P. J. M. Peters, P. Scheuzger, M. J. Lea, Yu. P. Monarkha, P. K. H. Sommerfeld, and R. W. van der Heijden, Phys. Rev. B **50**, 11 570 (1994).
[25] M. Seck and P. Wyder, Rev. Sci. Instrum. **69**, 1817 (1998).
[26] M. I. Dykman, M. J. Lea, P. Fozooni, and J. Frost, Phys. Rev. Lett. **70**, 3975 (1993); M. J. Lea, P. Fozooni, A. Kristensen, P.J. Richardson, K. Djerfi, M. I. Dykman, C. Fang-Yen, and A. Blackburn, Phys. Rev. B **55**, 16 280 (1997), and references therein.
[27] L. Wilen and R. Giannetta, J. Low Temp. Phys. **72**, 353 (1988).